scientific reports

Check for updates

OPEN

Unveiling Isorhapontigenin's therapeutic potential in lung cancer via integrated network pharmacology, molecular docking, and experimental validation

Zhiyu Wu[1,5,6], Chengyu Hou[2,3,6], Qiulin Zhu[2], Zixia Huang[2], Zesheng Lu[2,3], Chunhui Shen[1,5], Zhenhui Wang[1,5], Yanzhong Liu[1,5], Yanfen Kang[4]✉ & JiYong Wang[1,5]✉

Isorhapontigenin is an effective active ingredient in *Rheum officinale*, which has been reported to have anti-tumor effects. However, its effect and molecular mechanism on non-small cell lung cancer are still unclear. Firstly, potential therapeutic targets of Isorhapontigenin against non-small cell lung cancer were obtained through network pharmacology analysis. Secondly, bioinformatics analysis was conducted to identify key targets and potential signaling pathway mechanisms based on the obtained potential targets. Then, evaluated the binding ability between Isorhapontigenin and key targets by using molecular docking strategies. Finally, in vitro cell experiments were conducted to verify the effects and related targets of Isorhapontigenin on non-small cell lung cancer cells. 104 drug targets and 6688 disease targets were acquired from SwissTarget prediction, BATMAN-TCM, STITCH and Genecards databases.79 potential therapeutic targets were identified through analysis based on online Venn website and PPI interaction analysis was performed on these targets to ultimately obtain 55 key targets. GO and KEGG analysis revealed that Isorhapontigenin targets non-small cell lung cancer mainly through regulation of cell proliferation, cell cycle dynamics, and the PI3K/RELA/cell cycle axis. Molecular docking confirmed that Isorhapontigenin can bind to cell proliferation, cycle related proteins (*CCND1*, *CDK2*, *PIK3CA*, *RELA*). CCK-8 detection revealed that Isorhapontigenin significantly inhibited the proliferation of PC9 lung cancer cells, Moreover, RT-qPCR detection showed that Isorhapontigenin downregulated the expression of *CCND1*, *CDK2*, *PIK3CA* and *RELA* genes. *CCND1*, *CDK2*, *PIK3CA* and *RELA* are highly expressed in NSCLC tissues. Overall survival analysis of patients indicated that key genes in the *PIK3CA* and *NF-κBp65* signaling pathway significantly affected overall survival. Our research has found that Isorhapontigenin can effectively against non-small cell lung cancer, and this effect may be achieved by inhibiting cell proliferation and cycle progression mediated by the PIK3CA/NF-KB signaling pathway. Isorhapontigenin is a new potential therapeutic agent for lung cancer.

Keywords Isorhapontigenin, Non-small cell lung cancer, Network pharmacology, Bioinformatics, Molecular docking, Experimental verification, Cell cycle

Lung cancer is one of the most aggressive malignancies in terms of incidence and mortality. According to the 2022 global cancer burden statistics published in the authoritative international journal '*CA: A Cancer Journal for Clinicians*' in April 2024, lung cancer accounted for approximately 2.5 million new cases and 1.8 million deaths in 2024[1]. Non-small cell lung cancer (NSCLC) constitutes 85–90% of all lung cancer cases. Surgical resection remains the primary treatment for early- to mid-stage NSCLC in clinical practice. However, due to the insidious onset of lung cancer, most NSCLC patients are diagnosed at advanced stages, with over 81% missing

[1]The First Affiliated Hospital of Guangzhou University of Chinese Medicine, Guangzhou 510405, Guangdong, China. [2]Guangzhou University of Chinese Medicine, Guangzhou 510405, Guangdong, China. [3]Lingnan Medical Research Center of Guangzhou University of Chinese Medicine, Guangzhou 510405, Guangdong, China. [4]Department of Medicinal Oncology, The First Affiliated Hospital, Sun Yat-Sen University, Guangzhou 510080, China. [5]Guangdong Clinical Research Academy of Chinese Medicine, Guangzhou, Guangdong, China. [6]Zhiyu Wu and Chengyu Hou contributed equally to this work. ✉email: 1347115575@qq.com; 13802447736@139.com

the window for surgical intervention and nearly 70% requiring adjuvant therapies such as chemotherapy, targeted therapy, or immunotherapy post-surgery[2]. Although adverse effects of platinum-based chemotherapy, targeted therapies, and immunotherapies are milder than before, they remain widespread and profound, including myelosuppression, immunodeficiency, chemoradiotherapy-induced pneumonitis and dermatitis, and gastrointestinal complications. These significantly impair patients' survival outcomes and quality of life, with drug resistance inevitably emerging in later stages[3]. Therefore, developing more effective therapeutic strategies for NSCLC is urgently needed.

Traditional Chinese Medicine (TCM), with its unique theoretical framework and therapeutic approaches, has demonstrated distinctive advantages in cancer prevention and treatment. And there are more and more clinical evidences supporting the anti-cancer efficacy of TCM. In recent years, TCM has been widely reported to have good anti-cancer effects and has attracted increasing attention from researchers[4]. Some active ingredients in TCM such as quercetin, luteolin and kaempferol, have been shown to inhibit the growth of lung cancer cells[5–7].

Isorhapontigenin, a stilbenoid compound, exhibits anti-inflammatory, antioxidant, and *antitumor* activities. Modern studies have demonstrated its potent anticancer effects against various malignancies, including bladder cancer[8–11], prostate cancer[12], colorectal cancer[13], breast cancer[14], and glioblastoma[15]. For instance, Zhang et al. revealed that Isorhapontigenin suppresses bladder cancer cell migration and invasion by upregulating *METTL14* expression to reduce *vimentin* protein levels, thereby inhibiting epithelial-mesenchymal transition (EMT)[11]. Fang et al. reported that Isorhapontigenin inhibits specific protein 1 (*SP1*)-mediated transcriptional activation, downregulates cyclin D1 expression in bladder cancer cells, induces G_0-G_1 phase cell cycle arrest, and suppresses anchorage-independent cancer cell growth[16]. Zhu et al. demonstrated through in vitro and in vivo experiments that Isorhapontigenin significantly inhibits cell proliferation and induces apoptosis in prostate cancer by targeting *EGFR* and its downstream signaling pathways, including the *EGFR-PI3K-Akt* and *EGFR-Erk1/2* axes, while exerting minimal effects on normal prostate cells[12]. However, whether Isorhapontigenin exhibits therapeutic potential against NSCLC and its underlying molecular mechanisms remain unexplored.

Network pharmacology is a systematic pharmacology method, which is widely used in the study of TCM and their components' mechanisms of action[17]. By utilizing various databases of TCM and chemical components, network pharmacology can quickly identify potential targets and pathways of TCM against diseases and saving researchers or institutions a lot of experimental funds and valuable research time. At the same time, it also provides theoretical basis for subsequent in vitro and in vivo experiments. Molecular docking strategy is a computer simulation method that widely used in new drug development research[18]. With the help of molecular docking strategy, the binding possibility of drugs and their targets can be preliminarily determined, laying foundation for determining drug targets. In recent years, with the development of traditional Chinese medicine databases and computational biology, network pharmacology and molecular docking strategies have often been integrated for drug research.

In this study, we first used databases to obtain the therapeutic targets of Isorhapontigenin and NSCLC and further obtained the therapeutic targets of Isorhapontigenin through network pharmacology strategies. Then, we conducted bioinformatics analysis of key therapeutic targets, preliminarily validated some key targets through molecular docking strategies, and finally verified the efficacy and mechanism of Isorhapontigenin in treating NSCLC through in vitro cell experiments.

In summary, this study utilized network pharmacology analysis, in vitro experiments, and molecular docking to demonstrate that Isorhapontigenin effectively suppresses the progression of NSCLC cells. The underlying mechanism likely involves inhibition of the PIK3CA/NF-κB signaling pathway and its mediated cell proliferation and cell cycle. This research provides robust experimental evidence and theoretical support for Isorhapontigenin as a potential therapeutic agent for NSCLC. To our knowledge, this is the first study to report the therapeutic benefits of Isorhapontigenin in human NSCLC, significantly addressing a research gap in its application for lung cancer treatment.

The entire research process was shown in Fig. 1.

Materials and methods

Collection of Isorhapontigenin and NSCLC targets

The "Canonical SMILES" format of Isorhapontigenin was obtained by searching Isorhapontigenin in the PubChem database (https://pubchem.ncbi.nlm.nih.gov/), then it was inputted into the Swiss target prediction database for get potential targets. What is more, BATMAN-TCM (http://bionet.ncpsb.org.cn/batman-tcm/) and STITCH database (http://stitch-beta.embl.de/) were also used to acquire its potential targets. Finally, all targets of Isorhapontigenin obtained were consolidated in Excel, with duplicated genes removed. The targets related to NSCLC were obtained by searching the human gene database Genecards (https://www.genecards.org/).

Targets of Isorhapontigenin against NSCLC

The online Venn website (http://bioinformatics.psb.ugent.be/webtools/Venn/) was used to obtain potential targets for the treatment of NSCLC with Isorhapontigenin. The parameter conditions were set according to the default conditions of the website. After uploading drugs and disease targets, the website is run for online analysis to obtain online Venn map and potential target files.

Construction of PPI network and identification of key targets

In order to obtain the protein–protein interaction network (PPI) and core targets, potential therapeutic targets will be imported into the STRING database (https://www.string-db.org/) for protein–protein interaction analysis, with the species set as human and other parameter conditions set as default. Obtain a preliminary PPI file, then use the highest PPI score (confidence from 0.4 to 0.7) and remove disconnected targets in the network,

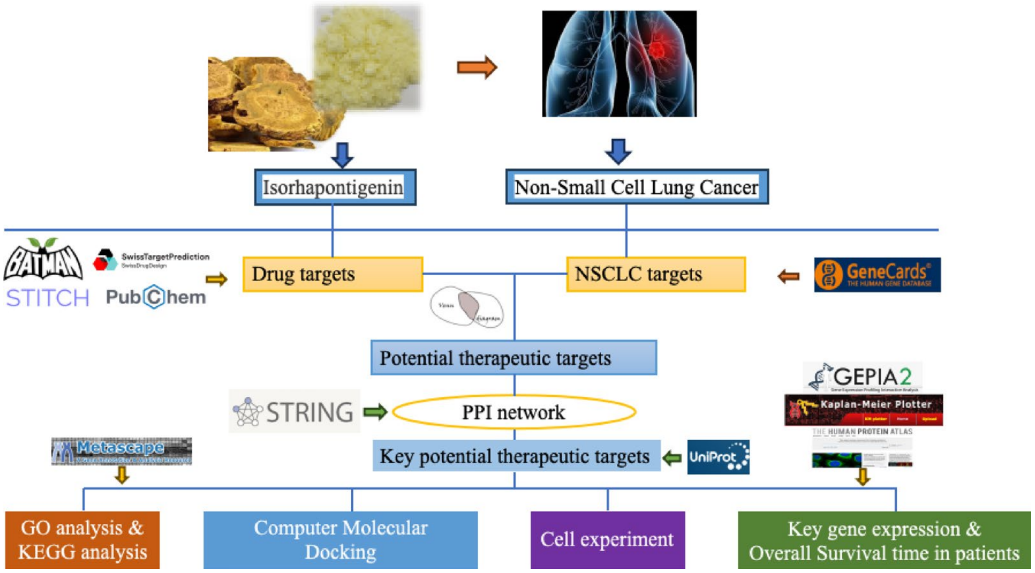

Fig. 1. This study first employed a network pharmacology approach to identify therapeutic targets for NSCLC and Isorhapontigenin. Key targets were then subjected to bioinformatics analyses, including KEGG and GO enrichment analyses, protein–protein interaction (PPI) network construction, and molecular docking, along with preliminary validation through immunohistochemistry and patient overall survival analysis. Finally, in vitro cellular experiments such as CCK-8 and RT-qPCR were performed to further validate the efficacy and mechanisms of Isorhapontigenin in NSCLC treatment.

and to obtain PPI of the core target. Finally, running the sorting script that installed in R software 4.0.2 to obtain sorting information for different core target based on network connectivity.

GO and KEGG enrichment analysis

The Metascape platform (https://metascape.org/) was used to analyze the final core therapeutic targets. The steps are briefly as follows. First, input the core targets into the gene list column of Metascape, then set the species as "Homo sapiens" with a P-value < 0.01, performing GO and KEGG enrichment analysis based on the core target. The data were sorted by p-value in ascending order, the top 10 entries were selected as significant terms, and the resulting image files were downloaded. Pathway analysis was conducted using the KEGG database[19–21], following the citation guidelines provided at http://www.kegg.jp/kegg/kegg1.html. GO enrichment analysis includes Biological Process (BP), Cellular Component (CC), Molecular Function (MF).

Molecular docking

Select core proteins from the core targets and key signaling pathways for molecular docking to preliminarily validate the core functional targets of Isorhapontigenin. As mentioned above, Retrieve Isorhapontigenin in the Pubchem database and download small molecule ligand 3D structures (3D Conformers) with SDF format, then using open babel 3.1.1 to convert the SDF format of small molecule ligands to mol2 format. Obtain the protein 3D structure in the RCSBPDB database (https://www.uniprot.org/), the limiting condition was set to human protein and small molecule ligand information in the structural complex. After downloading the PDB format, remove water molecules and small molecule ligands using Pymol 2.4.0 software and save the PDB format as the receptor protein. Perform hydrogenation and other processing on protein receptors and small molecule ligands in Autodock 1.5.6 software, save them as PDBQT format files, set appropriate docking boxes and parameters, use Autodock Vina 1.1.2 for molecular docking, save the results, and select some results for visual analysis in Pymol. If the binding energy score is less than or equal -5, it indicates that the ligand and receptor can bind well.

Cell experiments

CCK-8 assay

Isorhapontigenin (98% purity HPLC) was purchased from Alfa Biotechnology Co.Ltd (Chengdu,China). It was dissolved in DMSO (Sigma,USA) to a concentration of 100 mM/L mother liquor for later use. PC9 lung cancer cells were purchased from Noble Biological Products Co.Ltd (Nobcell 0415, Hangzhou, China). PC9 cells were cultured in DMEM medium containing 10% FBS, penicillin (100 U/mL) and streptomycin (0.1 mg/mL) in an incubator at 37 °C and 5% CO_2. The medium was changed every 2–3 days, and passage was performed when the cell fusion reached 90%. After the cells were fully grown, they were seeded and cultured in a 96-well cell culture plate with approximately 8000 cells per well. After 24 h of cell adhesion, they were observed under microscope. Then different concentrations of drugs were used to intervene in the cells for 24 and 48 h. After intervention, the culture medium was discarded and 110 ul culture medium (containing 10 ul of CCK-8 solution, fetal bovine serum free) was added to each well. CCK-8 reagent was purchased from Suzhou Xinsaimei

Biotechnology Co., Ltd. After incubating CCK-8 for 1 h, the OD value was detected at 450 nm by microplate reader (Thermo Fisher,USA), the drug concentration that meets the IC50 condition is considered for subsequent cell experiments.The IC50 value of Isorhapontigenin was calculated using GraphPad Prism 9.0 software. Drug concentrations and their corresponding relative cell viability values were imported into the software. The analysis was performed by selecting "[inhibitor] vs. Normalized Response—Variable slope" under "Nonlinear regression (curve fit)", and the IC50 value was subsequently determined.

Real time fluorescence quantitative PCR assay

According to the CCK-8 results, the cell inoculation and intervention for RT-qPCR experiments were performed. After cell intervention, the culture medium was discarded and the cells were washed twice with PBS (Gibco, USA). Total RNA was extracted from cells using the Trizol reagent according to the manufacturer's instructions. The purity and concentration of RNA were detected by a spectrophotometer (Thermo Fisher,USA). RNA with a purity of at least 1.7 was used for subsequent experiments. The obtained RNA was reverse transcribed into cDNA using reverse transcription kit (Takara,Japan). cDNA, SYBR Premix Ex TaqTM II (Tli RNaseH Plus)(Takara) and primers were added to 96-well well plates for amplification. RT-qPCR conditions were predenaturation at 95 °C for 10 min, denaturation at 95 °C for 15 s, annealing at 60 °C for 30 s, and a total of 40 cycles were performed. The relative expression of each gene was calculated by $2^{-\Delta\Delta CT}$ method. The relevant primer sequences are as shown in the Table 1 below.

Validation of key targets in HPA database

The protein expression and distribution of *CCND1, CDK2, PIK3CA and RELA* in normal lung and NSCLC tissues were searched in the HPA database (https://www.proteinatlas.org/).

Gene expression level analysis

Expression levels of the selected key genes are analyzed using the Gene Expression Profiling Interactive Analysis (GEPIA) database (http://gepia2.cancer-pku.cn/#survival). The "Gene Expression Profile" option is selected, with a Log_2 FC cutoff of "1" and a p-value cutoff of "0.01," choosing the disease type as "NSCLC" and selecting "Match TCGA normal and GTEx data" for Matched Normal data. The expression levels of the *CCND1, CDK2, PIK3CA* and *RELA* genes in NSCLC tissues compared to normal tissues are obtained and presented as Box Plots.

Overall survival analysis of patients

The overall survival of NSCLC patients is analyzed using the GEPIA database and the Kaplan–Meier Plotter (KM Plotter) database (https://kmplot.com/analysis/). Key genes are retrieved separately in both GEPIA and KM Plotter databases, with high and low expression rates set at 50% and the disease type selected as "NSCLC" Ultimately, survival curves for key genes in the *CCND1, CDK2, PIK3CA* and *RELA* signaling pathway among NSCLC patients are plotted.

Statistical analysis

Experimental data were analyzed using GraphPad Prism 9.0 software. Before performing ANOVA for multi-group comparisons or t-tests for pairwise comparisons, normality and homogeneity of variance were tested. Only data meeting normality and homogeneity of variance criteria were subjected to ANOVA or t-tests. For multi-group comparisons violating homogeneity of variance, Brown-Forsythe test was used to assess overall differences, followed by Tamhane's T2 post hoc test for pairwise comparisons. Statistical significance was denoted as: *($P<0.05$), **($P<0.01$), ***($P<0.001$), and ****($P<0.0001$). All experiments were repeated at least three times.

Results

Collection of targets for Isorhapontigenin and NSCLC

To obtain the therapeutic targets of NSCLC and Isorhapontigenin, we searched for potential targets of Isorhapontigenin from SwissTarget prediction, BATMAN-TCM, and STITCH databases, and obtained a total of 104 drug-related targets after deduplication. As shown in Fig. 2, the 2D structure of Isorhapontigenin from PubChem database. 6688 NSCLC related targets were obtained from the Genecards database.

Potential targets and PPI network of Isorhapontigenin against NSCLC

We identified the shared therapeutic targets between NSCLC and Isorhapontigenin. With the help of the online Venn analysis website, drug and disease-related targets were analyzed, as shown in Fig. 3, a total of 79 potential

Primers	Forward	Reverse
Human *GAPDH*	CCAGCAAGAGCACAAGAGGA	TGAGGAGGGGAGATTCAGTGT
Human *CCND1*	TGAGGGACGCTTTGTCTGTC	CTTCTGCTGGAAACATGCCG
Human *CDK2*	GACACGCTGCTGGATGTCA	GAGGACCCGATGAGAATGGC
Human *PIK3CA*	AAGAGCCCCGAGCGTTT	ACTAGGATTCTTGGGGGCAT
Human *RELA*	CCTTCCAAGAAGAGCAGCGTG	CTGCCAGAGTTTCGGTTCAC

Table 1. Primer sequences.

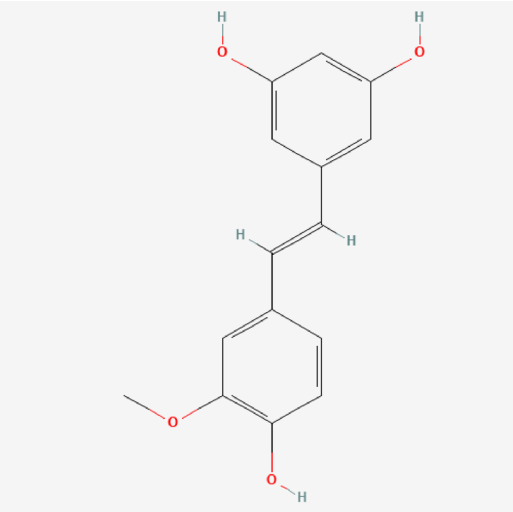

Fig. 2. the 2D structure of Isorhapontigenin, CAS number 32507-66-7.

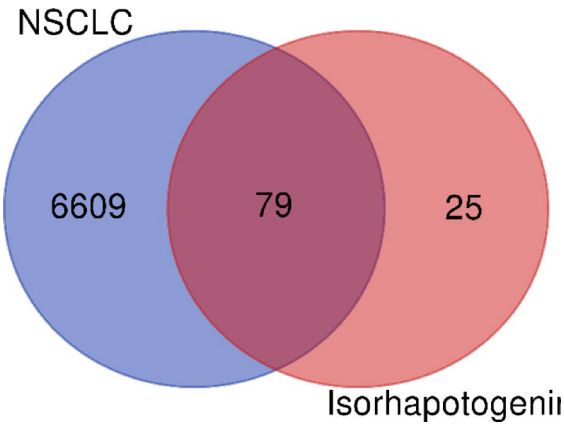

Fig. 3. 79 potential targets of Isorhapontigenin against NSCLC were identified by online Venn website.

targets were obtained by taking intersection. The 79 target proteins were imported into the STRING database to obtain protein- protein interaction network, as shown in Fig. 4.

Key targets and PPI network of Isorhapontigenin against NSCLC

In order to further screen the core target proteins, the STRING database function module was used to set the highest confidence level (0.7) and hide the disconnected targets. Finally, 55 key target proteins were obtained and their PPI network were plotted, as shown in Fig. 5. Based on network connectivity, R software was performed to sort targets in network, as shown in Fig. 6, the key targets such as *SRC, STAT3, PIK3CA, ESR1, IGF1R, CDK1, CDK 2, BCL2, RELA* were finally identified.

GO enrichment analysis of key targets

GO enrichment analysis was performed by Metascape platform, as shown in Figs. 7, 8 and 9. The biological processes involved in the enrichment of 55 key genes are as follows: response to xenobiotic stimulus, oxidative stress, regulation of inflammatory response, cell population proliferation, etc. Gene products are mainly enriched in nuclear envelope, cell body, membrane raft, receptor complex, etc. Molecular functions mainly focus on protein kinase activity, heme binding, protein domain specific binding, protein tyrosine kinase activity, etc. NSCLC exhibits close associations with biological processes, molecular functions, and cellular components identified through GO enrichment analysis: Activation of xenobiotic metabolic genes (e.g., cytochrome P450) may drive chemoresistance, while oxidative stress promotes tumor progression via ROS-mediated DNA damage and KRAS/EGFR mutations. Chronic inflammation (IL-6/STAT3 and TNF-α/NF-κB pathways) and dysregulated proliferative signaling (EGFR/ALK/PI3K pathways) synergistically drive malignant transformation and metastasis. Among critical cellular components, aberrant nuclear envelope proteins (e.g., Lamin A/C) compromise DNA repair, whereas membrane raft-enriched receptors (EGFR, HER2) and mutant receptor complexes (e.g., EGFR-L858R) sustain activation of downstream kinase signaling (MAPK/ERK).

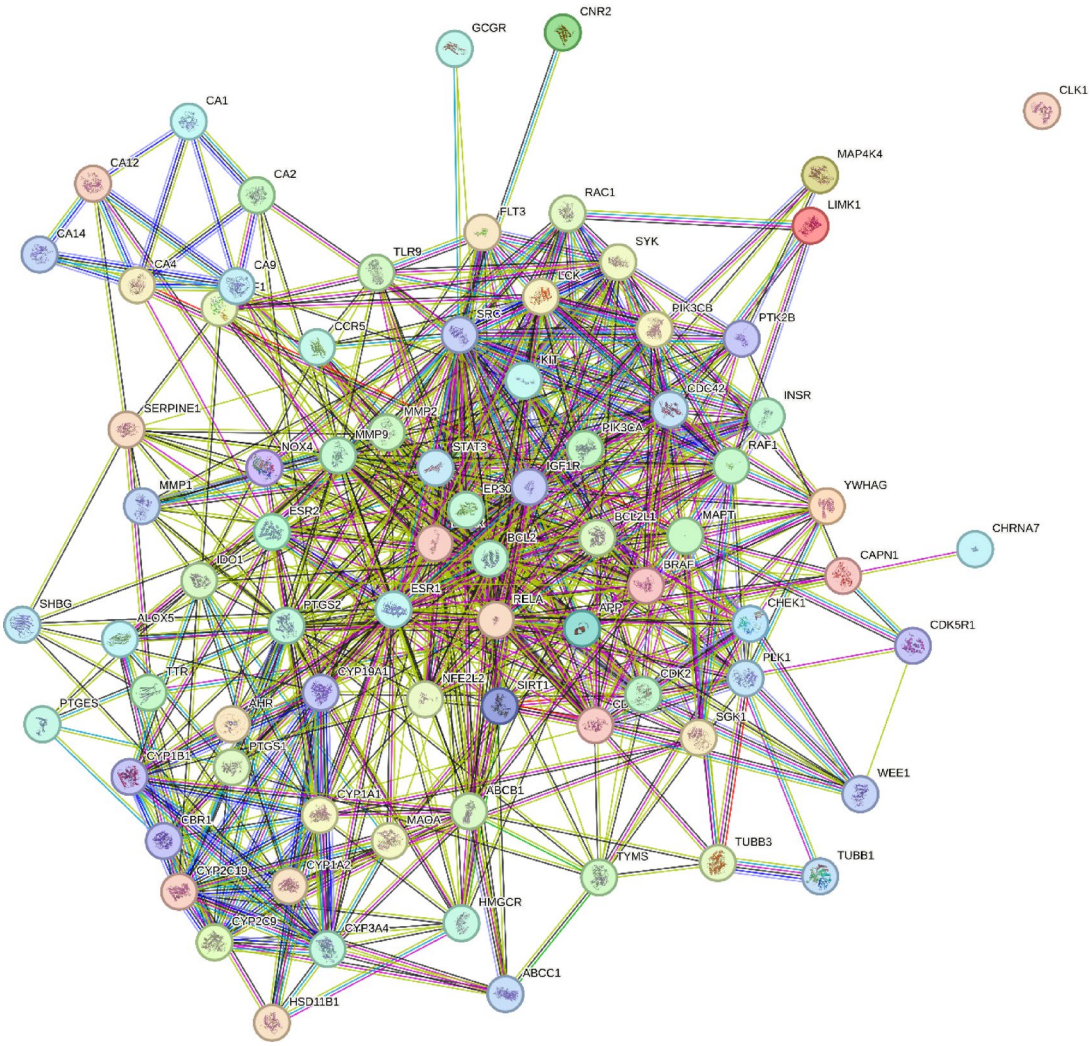

Fig. 4. PPI network of 79 targets protein that Isorhapontigenin against NSCLC. Each circular dot represents a node, denoting a protein, while the connecting lines indicate the interaction relationships between proteins, with different colors corresponding to distinct types of interactions.

At the molecular functional level, abnormal activation of protein kinases (EGFR, ALK) and heme-binding proteins (HO-1) respectively constitute focal targets for tyrosine kinase inhibitors (TKIs) and antioxidant-based therapeutic interventions.

KEGG enrichment analysis of key targets

KEGG enrichment analysis was also based on the Metascape platform. As shown in Fig. 10, KEGG enrichment analysis, found that the 55 potential key targets of Isorhapontigenin against NSCLC were mainly enriched in the cancer pathway, PI3K/AKT signaling pathway, cell cycle pathway, NF-κB signaling pathway.

Molecular docking analysis

Molecular docking was performed using Autodock Vina 1.1.2 software. *PIK3CA, CDK2, RELA*, and the cell proliferation-related protein *CCND1* were selected as molecular docking targets based on their critical roles in the protein–protein interaction (PPI) network, KEGG enrichment analysis results, and cell proliferation cycle phenotypes. As demonstrated in Table 2, the binding energy scores indicate that all four proteins exhibit favorable binding affinities with Isorhapontigenin, with particularly significant interactions observed for *PIK3CA* and *CDK2* proteins. Detailed molecular docking visualization results for these four targets are presented in Figs. 11, 12, 13 and 14.

Isohesperidin significantly inhibited the proliferation activity of PC9 cells

As demonstrated in Fig. 15, PC9 cells treated with varying concentrations of Isorhapontigenin for 24 and 48 h exhibited concentration- and time-dependent inhibition of cell proliferation. The calculated IC50 value was 75.84 μM. The most potent inhibitory effect was observed at 100 μM, with approximately 50% inhibition achieved after 48 h of treatment. Based on the concentration gradient design and to ensure experimental consistency

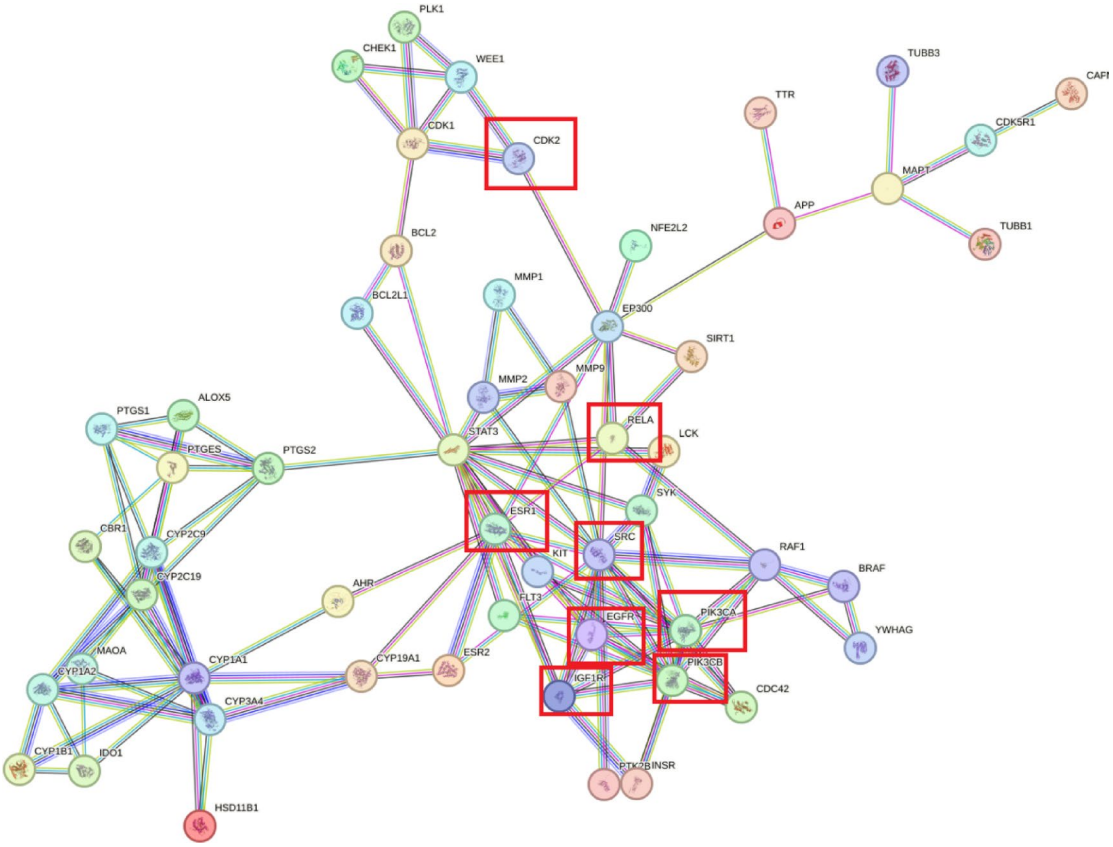

Fig. 5. PPI network of key targets protein that Isorhapontigenin against NSCLC (hide disconnected targets). Each circular node represents a protein, with connecting lines indicating protein–protein interaction relationships, where distinct colors correspond to different types of interaction mechanisms.

and facilitate subsequent data analysis, 100 μM combined with a 48-h treatment duration was selected as the standardized experimental condition for further investigations.

Isohesperidin may induce proliferation inhibition and cell cycle arrest of PC9 cells by inhibiting the PI3K/NF-κB signaling pathway

After 48 h of drug intervention in PC9 cells, RT-qPCR analysis showed that (as shown in Fig. 16), the expression levels of key genes of cell proliferation and cycle (*CCND1, CDK2*) were significantly downregulated, and the expression levels of key genes in the PI3K/NF-KB signaling pathway (*PIK3CA, RELA*) of NSCLC cell proliferation were also significantly downregulated $^{**}P < 0.01$, The difference was statistically significant.

Immunohistochemical staining was performed for key genes of *CCND1*, *CDK2*, *PIK3CA* and *RELA* based on HPA database

To investigate the immunohistochemical staining profiles of *CCND1*, *CDK2*, *PIK3CA*, and *RELA* genes in NSCLC, we utilized the HPA database. In the HPA database, gene expression analysis revealed the following: *CCND1* was evaluated in 17 patient samples (14 lung cancer tissues vs. 3 normal lung tissues); *CDK2* was analyzed in 14 samples (11 lung cancer tissues vs. 3 normal lung tissues); *PIK3CA* was assessed in 15 samples (12 lung cancer tissues vs. 3 normal lung tissues); *RELA* was examined in 15 samples (12 lung cancer tissues vs. 3 normal lung tissues). The results demonstrated a statistically significant increase in the expression levels of *CCND1, CDK2, PIK3CA,* and *RELA* in NSCLC tissues compared to normal lung tissues (Fig. 17).

Differences in the expression of *CCND1*, *CDK2*, *PIK3CA* and *RELA* genes in lung cancer tissues and normal lung tissues and their effects on overall survival of patients

To investigate the expression levels of key genes in the PIK3CA and NF-kB p65 (encoded by the *RELA* gene) signaling pathways in NSCLC patients and their impact on overall survival, we analyzed the expression levels of *CCND1, CDK2, PIK3CA,* and *RELA* in NSCLC tissues and normal lung tissues using the GEPIA and Kaplan–Meier databases. We further examined the overall survival of NSCLC patients under high and low expression conditions (50% each) for *CCND1, CDK2, PIK3CA,* and *RELA* (Figs. 18 and 19). The results showed that, compared to normal tissues, the expression of *CCND1, CDK2, PIK3CA,* and *RELA* was higher in NSCLC tissues. Additionally, NSCLC patients with lower expression levels of *CCND1, CDK2, PIK3CA,* and *RELA* exhibited

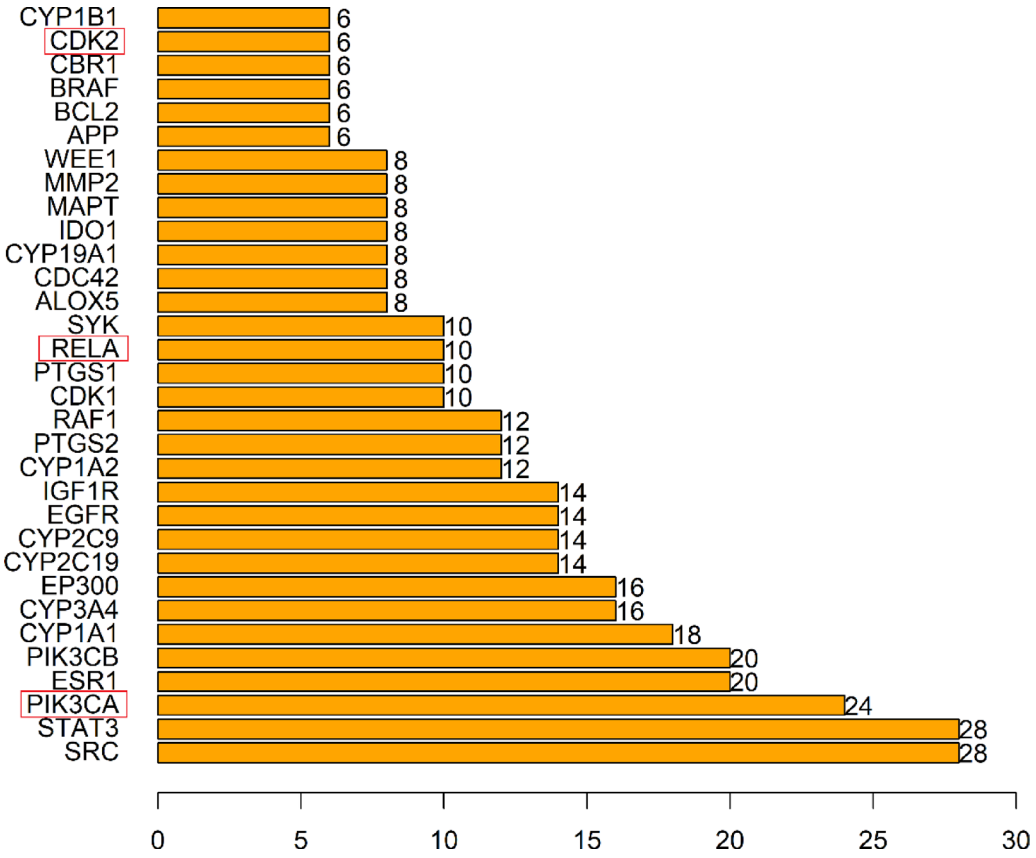

Fig. 6. the rank of key targets protein that Isorhapontigenin against NSCLC based on network connectivity. Using the R programming language, the genes in the PPI network were sorted in ascending order based on their node centrality metrics.

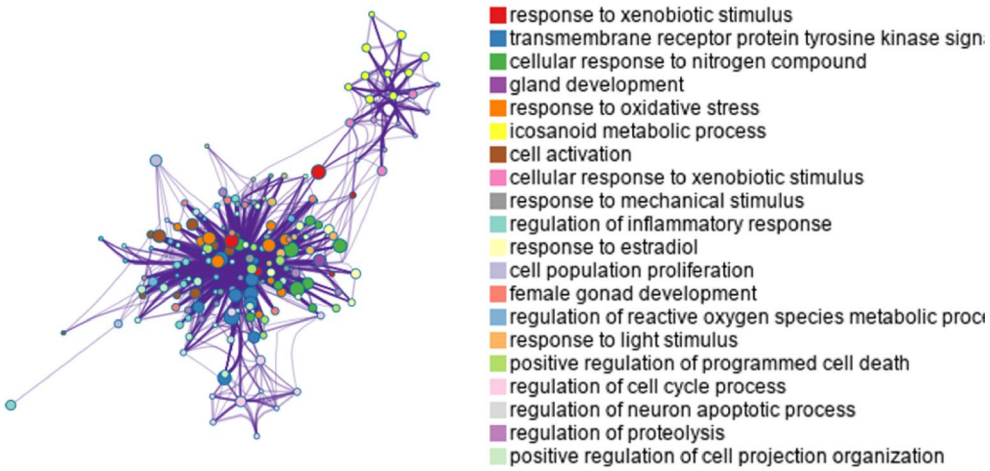

Fig. 7. BP Results from GO Enrichment Analysis of the 55 Key Targets.

longer overall survival compared to the control group. This suggests that these targets may play a critical role in extending the overall survival of NSCLC patients.

Discussion

NSCLC has influenced a large number of patients and poses a great threat to them, seriously reduce the quality of life of patients and increasing the burden of social medical care. To date, effective drugs for treating NSCLC remain limited. TCM has shown growing promise in tumor non-surgical treatment. Recent large-scale clinical studies on specific TCM prescriptions have significantly advanced cancer drug research[22].

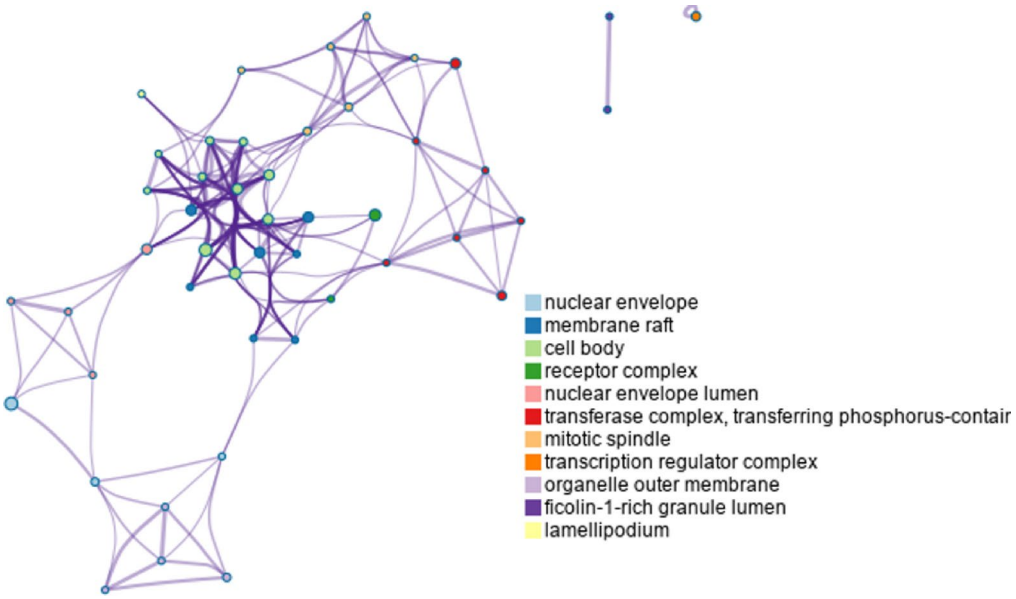

Fig. 8. CC Results from GO Enrichment Analysis of the 55 Key Targets.

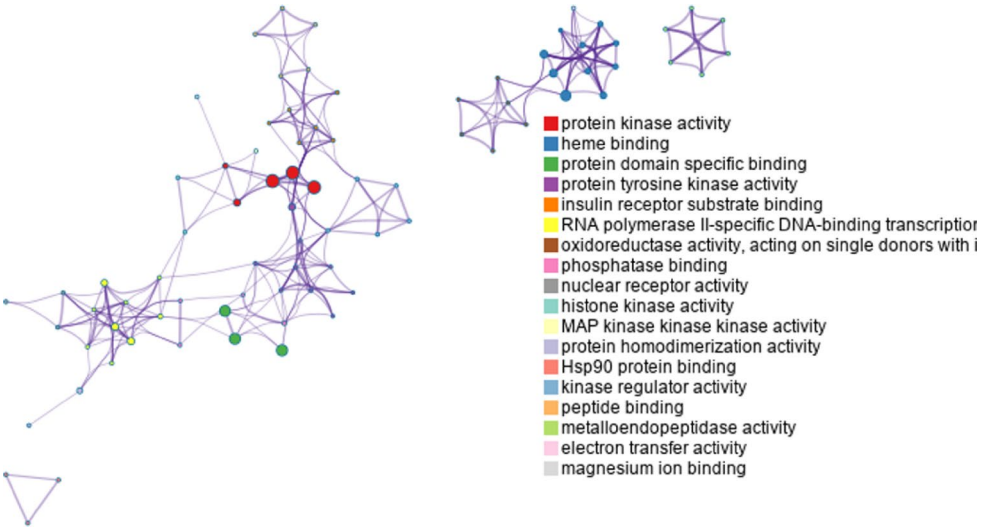

Fig. 9. MF Results from GO Enrichment Analysis of the 55 Key Targets.

Modern pharmacological evidence confirms Isorhapontigenin possess notable anticancer properties[23,24]. In this study, we combined network pharmacology, bioinformatics, molecular docking, and in vitro experiments to investigate Isorhapontigenin's anti-NSCLC mechanisms.

Our integrated methodology offers distinct advantages for drug discovery. Through network pharmacology databases, we identified 104 Isorhapontigenin targets and 6688 NSCLC-related targets, ultimately pinpointing 55 key therapeutic targets. Notably, STAT3, ESR1, SRC and EGFR among them are well-documented in NSCLC pathogenesis[25–28]. Subsequent molecular docking revealed strong binding affinity between Isorhapontigenin and critical proteins: cell cycle regulators (*CCND1, CDK2*) and signaling molecules (*PIK3CA, NF-κBp65/RELA*). These findings suggest Isorhapontigenin may inhibit NSCLC proliferation through cell cycle arrest and PI3K/NF-κB pathway modulation.

The PI3K/Akt/NF-κB signaling pathway is a key focus in cancer research[29,30] and plays a significant role in NSCLC. PI3K, an intracellular phosphatidylinositol kinase, comprises a regulatory subunit (p85) and a catalytic subunit (p110). Upon ligand binding to membrane receptors, the receptor activates p85, recruiting p110 to catalyze the conversion of phosphatidylinositol 4,5-bisphosphate (PIP2) to phosphatidylinositol 3,4,5-trisphosphate (PIP3) on the inner membrane surface, thereby activating Akt. Activated Akt translocates to the cytoplasm and nucleus, where it is phosphorylated to regulate downstream targets, modulating diverse cellular functions. Notably, *PIK3CA* encodes the p110 catalytic subunit of PI3K and is a critical kinase in the

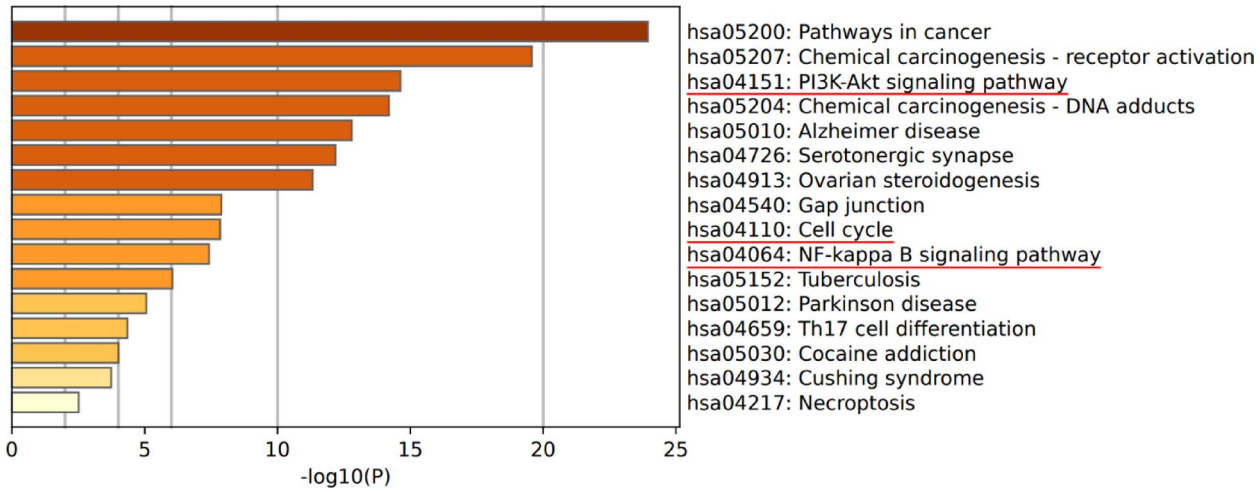

Fig. 10. Results of KEGG Enrichment Analysis for the 55 Key Targets. The bar length represents the number of targets enriched in each signaling pathway, while the color gradient of the bars (from light yellow to dark brown) corresponds to the magnitude of the P-value, with lighter shades indicating lower P-values and darker shades indicating higher significance. The KEGG images were constructed as per the citation guidelines: www.kegg.jp/kegg/kegg1.html.

Drug	Protein	ID	Resolution ratio	Ligand	Binding energy(kj/mol)	RMSD
Isorhapontigenin	*CCND1*	6P8E	2.3 A	–	− 6.3	0.744
Isorhapontigenin	*CDK2*	3PXQ	1.9 A	–	− 8.0	0.692
Isorhapontigenin	*PIK3CA*	7R9V	2.69 A	–	− 8.6	0.683
Isorhapontigenin	*RELA*	9BDV	1.9 A	–	− 7	0.81

Table 2. The molecular binding energy between Isorhapontigenin and *CCND1*, *CDK2*, *PIK3CA*, and *RELA*.

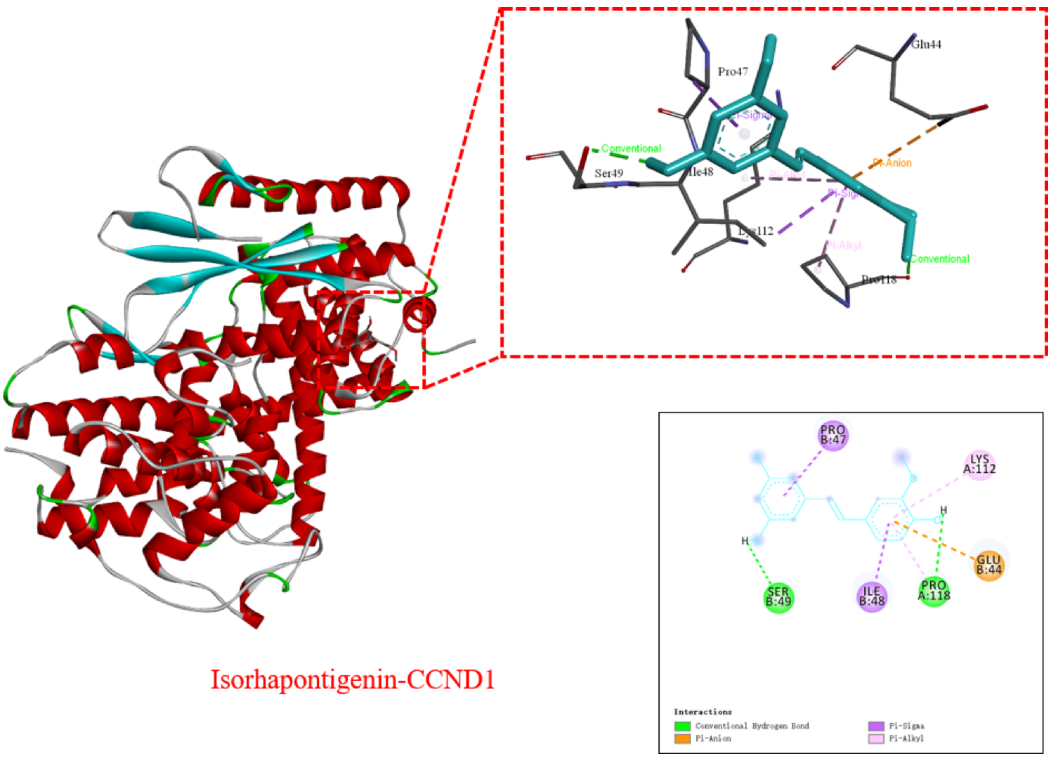

Fig. 11. Visualization diagram of molecular docking between Isorhapontigenin and *CCND1*.

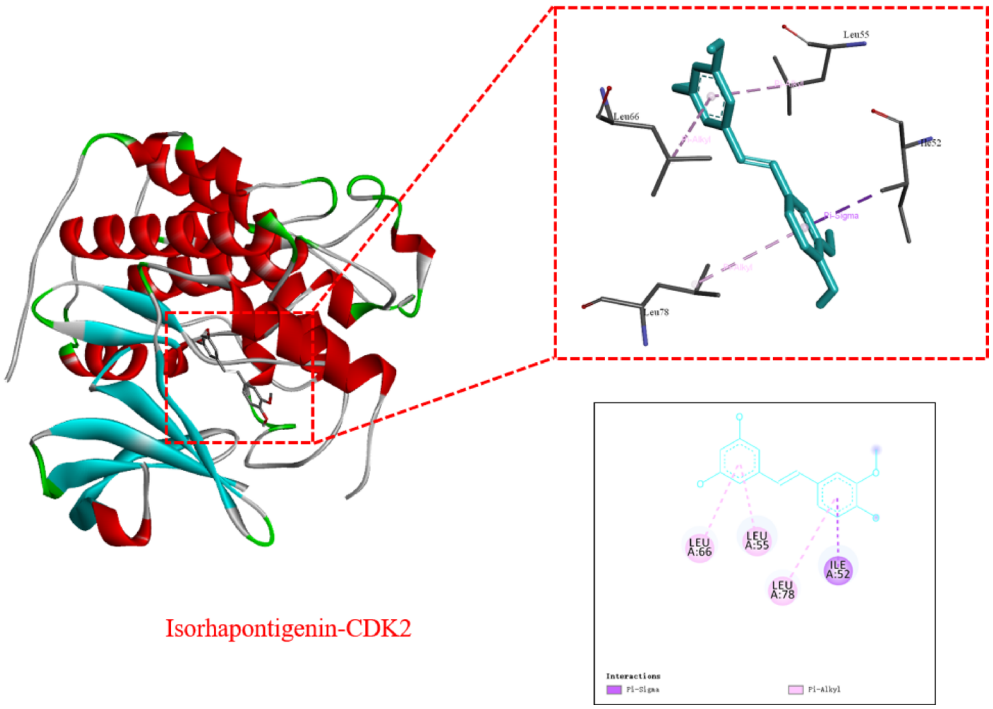

Fig. 12. Visualization diagram of molecular docking between Isorhapontigenin and *CDK2*.

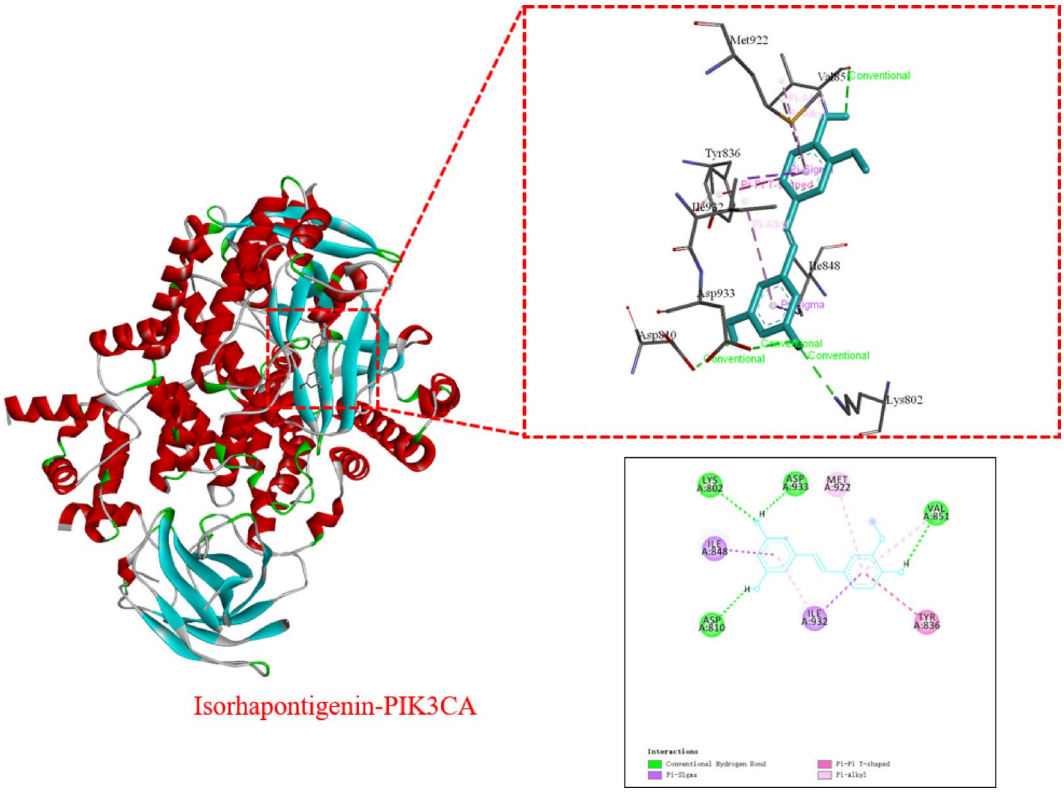

Fig. 13. Visualization diagram of molecular docking between Isorhapontigenin and *PIK3CA*.

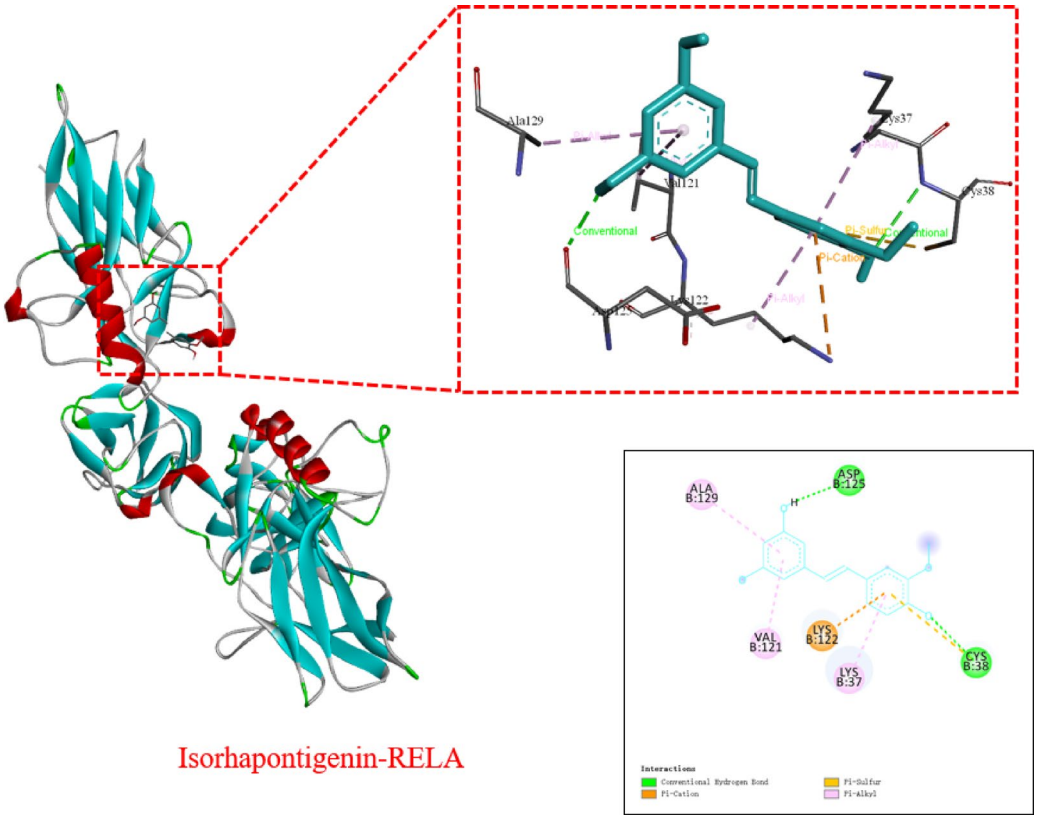

Fig. 14. Visualization diagram of molecular docking between Isorhapontigenin and *RELA*.

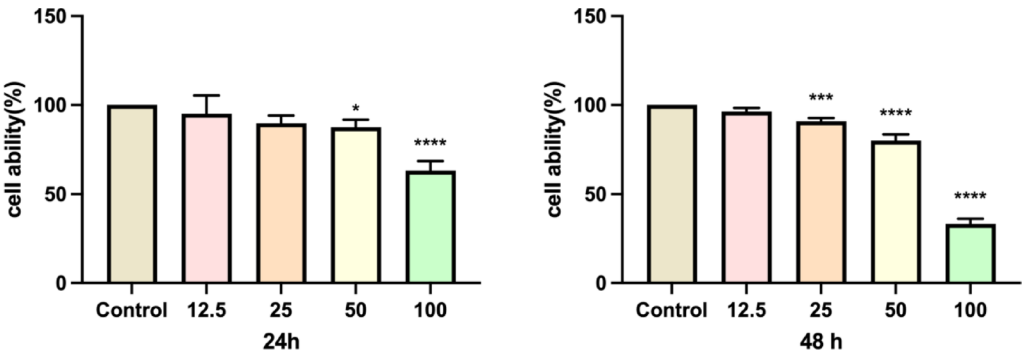

Fig. 15. CCK-8 assay of PC9 cell viability after 24- and 48-h treatment with Isorhapontigenin ($n = 4$ biological replicates). Compared to the Control group, Isorhapontigenin exhibited concentration- and time-dependent inhibition of PC9 cell activity. * indicates $P < 0.05$, ** indicates $P < 0.01$, *** indicates $P < 0.001$, **** indicates $P < 0.0001$.

PI3K/Akt pathway[31–33]. Studies indicate that PI3K activation in NSCLC induces Akt phosphorylation, which promotes the degradation of IκB, enabling nuclear translocation of NF-κB and subsequent transcription of pro-survival target genes (Fig. 1). NF-κB activation further upregulates intercellular adhesion molecule-1 (ICAM-1) and induces matrix metalloproteinase-9 (MMP-9) expression, driving tumor proliferation and invasion[34].

In NSCLC, cisplatin has been shown to activate Akt in A549 lung adenocarcinoma cells, and blocking the PI3K/Akt pathway enhances cisplatin-induced apoptosis while reducing cell viability. NF-κB, a downstream effector of PI3K/Akt, is suppressed by baicalein, a flavonoid that sensitizes A549 cells to cisplatin by inhibiting the PI3K/Akt/NF-κB axis[35].

In conclusion, the PI3K/Akt/NF-κB pathway is pivotal in NSCLC progression and represents a therapeutic target. Its inhibition can counteract key oncogenic mechanisms, highlighting its potential in anti-cancer strategies.

In vitro validation demonstrated dose/time-dependent suppression of PC9 cell proliferation via CCK-8 assays. RT-qPCR confirmed Isorhapontigenin significantly downregulated *CCND1, CDK2, PIK3CA* and *RELA* expression,

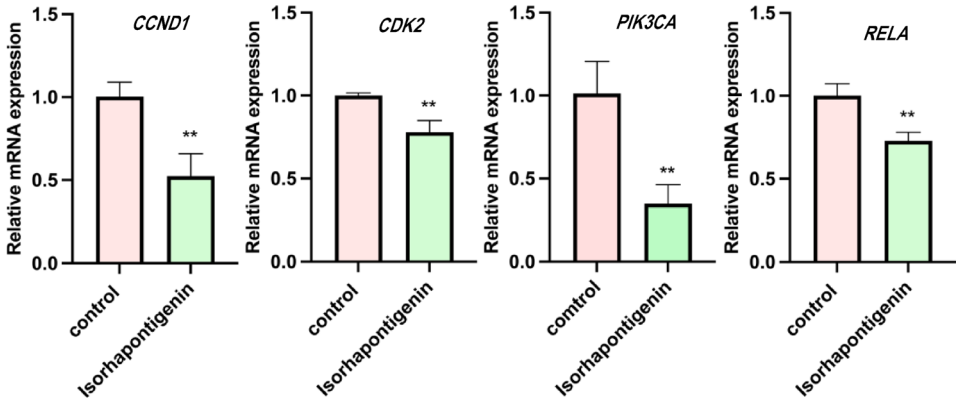

Fig. 16. RT-qPCR analysis of *CCND1*, *CDK2*, *PIK3CA*, and *RELA* gene expression levels in PC9 cells following 48-h treatment with Isorhapontigenin ($n = 3$ biological replicates). Compared to the Control group, the Isorhapontigenin-treated group exhibited decreased relative mRNA expression levels of all tested genes (*CCND1*, *CDK2*, *PIK3CA*, and *RELA*). * indicates $P < 0.05$, ** indicates $P < 0.01$, *** indicates $P < 0.001$, **** indicates $P < 0.0001$.

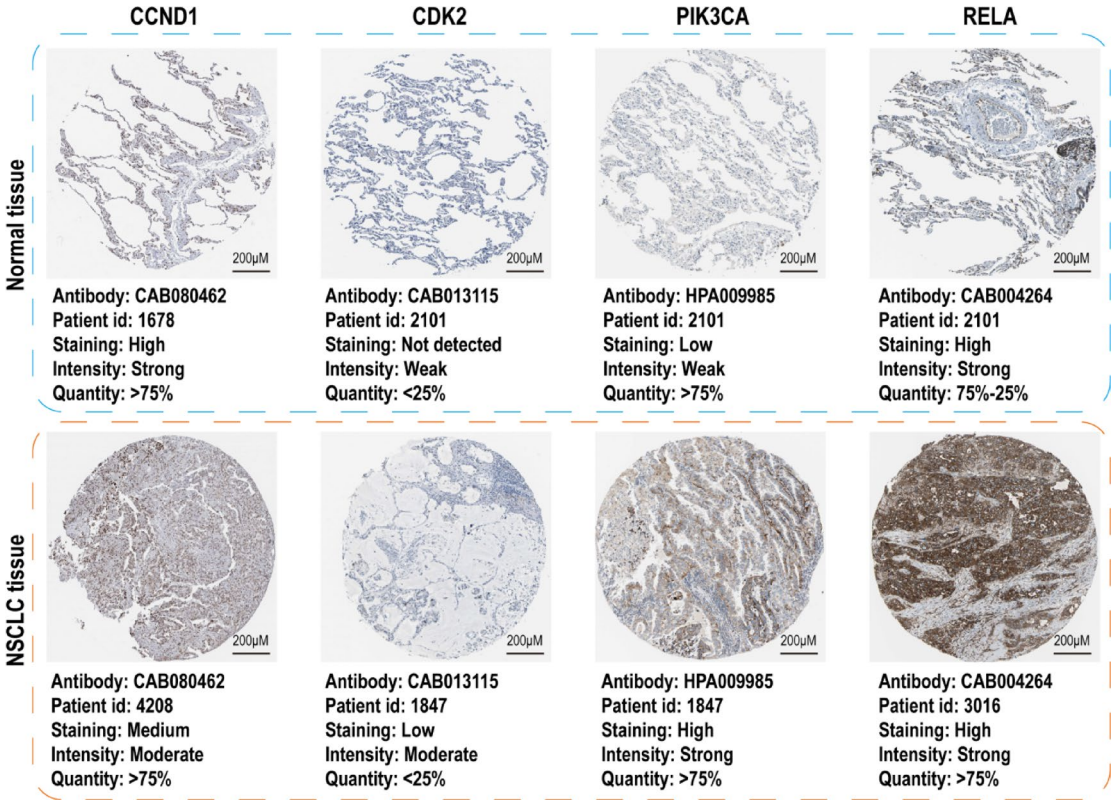

Fig. 17. In the HPA database, we performed targeted queries for the *CCND1* (n = 17), *CDK2* (n = 14), *PIK3CA* (n = 15), and *RELA* (n = 15) genes to compare their expression levels and immunohistochemical staining intensity between normal lung tissues and NSCLC tissues.

compared with the control group, ** denotes $P < 0.01$, indicating a statistically significant difference. These targets hold distinct pathological significance: CCND1/CDK2 regulate cell cycle progression[36,37]; PIK3CA activates PI3K/AKT signaling[32]; *RELA*-encoded NF-κBp65 mediates both PI3K/AKT and NF-κB pathways, influencing tumor microenvironment[38,39]. HPA database pathological data corroborated their overexpression in NSCLC tissues. Survival analysis further indicated lower expression levels correlate with improved patient prognosis.

Our study has several limitations. First, the limited clinical sample size may restrict the generalizability of our findings. Additionally, further investigation is warranted to determine whether *CCND1*, *CDK2*, *PIK3CA*, and *RELA* directly regulate cell cycle progression in this context. The mechanisms by which Isorhapontigenin modulates the

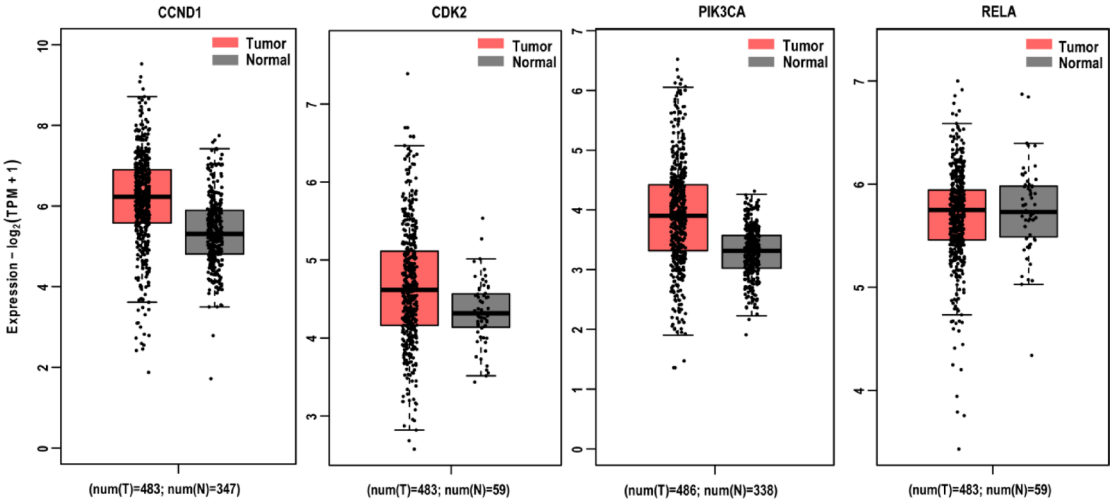

Fig. 18. In the GEPIA database, we conducted individual *queries* for *CCND1, CDK2, PIK3CA, and RELA* to compare their expression levels in NSCLC tumor tissues and normal lung tissues. Tumor tissues are represented in red and normal tissues in gray.

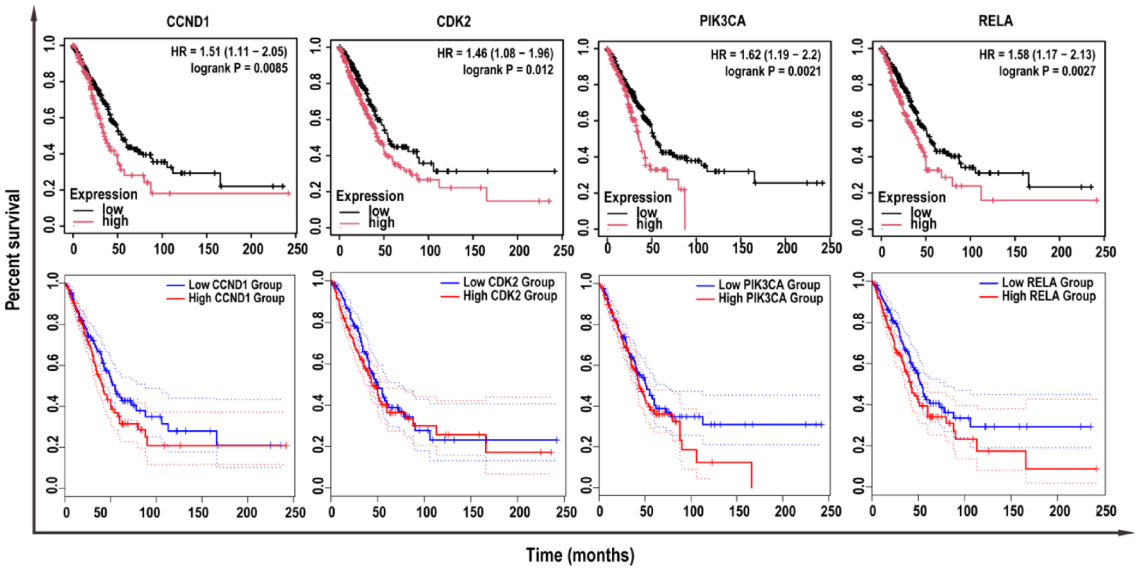

Fig. 19. In the GEPIA and KM Plotter databases, we analyzed differences in overall survival between high-expression and low-expression groups (stratified by median expression values, each constituting 50% of the cohort) of the *CCND1*, *CDK2*, *PIK3CA*, and *RELA* genes in NSCLC patients.

PI3K/NF-κB signaling pathway—and whether it exerts anti-lung cancer effects through other pathways—require further mechanistic exploration.

Current experimental evidence suggests that isorhapontigenin may suppress lung cancer progression via inhibition of the PI3K/NF-κB axis, though its precise molecular targets and broader regulatory networks remain to be elucidated.

Data availability

The datasets presented in this study can be found in online repositories. The names of the repository/repositories and accession number(s) can be found in the article/supplementary material.

Received: 27 February 2025; Accepted: 7 May 2025
Published online: 29 May 2025

References

1. Bray, F. et al. Global cancer statistics 2022: GLOBOCAN estimates of incidence and mortality worldwide for 36 cancers in 185 countries. *CA Cancer J. Clin.* **74**, 229–263. https://doi.org/10.3322/caac.21834 (2024).
2. Copur, M. S. State of cancer research around the globe. *Oncology (Williston Park)* **33**, 181–185 (2019).
3. Zheng, R. S. et al. Cancer incidence and mortality in China, 2022. *Zhonghua Zhong Liu Za Zhi* **46**, 221–231. https://doi.org/10.3760/cma.j.cn112152-20240119-00035 (2024).
4. Li, Z., Feiyue, Z. & Gaofeng, L. Traditional Chinese medicine and lung cancer–From theory to practice. *Biomed. Pharmacother.* **137**, 111381. https://doi.org/10.1016/j.biopha.2021.111381 (2021).
5. Alsharairi, N. A. Quercetin derivatives as potential therapeutic agents: An updated perspective on the treatment of nicotine-induced non-small cell lung cancer. *Int. J. Mol. Sci.* https://doi.org/10.3390/ijms242015208 (2023).
6. Jiang, Z. Q. et al. Luteolin inhibits tumorigenesis and induces apoptosis of non-small cell lung cancer cells via regulation of MicroRNA-34a-5p. *Int. J. Mol. Sci.* https://doi.org/10.3390/ijms19020447 (2018).
7. Wang, R. et al. Kaempferol promotes non-small cell lung cancer cell autophagy via restricting Met pathway. *Phytomedicine* **121**, 155090. https://doi.org/10.1016/j.phymed.2023.155090 (2023).
8. Hua, X. et al. Induction of RAC1 protein translation and MKK7/JNK-dependent autophagy through dicer/miR-145/SOX2/miR-365a axis contributes to isorhapontigenin (ISO) inhibition of human bladder cancer invasion. *Cell Death Dis.* **13**, 753. https://doi.org/10.1038/s41419-022-05205-w (2022).
9. Luo, Y. et al. Isorhapontigenin (ISO) inhibits stem cell-like properties and invasion of bladder cancer cell by attenuating CD44 expression. *Cell Mol. Life Sci.* **77**, 351–363. https://doi.org/10.1007/s00018-019-03185-3 (2020).
10. Kowalczyk, T., Piekarski, J., Merecz-Sadowska, A., Muskała, M. & Sitarek, P. Investigation of the molecular mechanisms underlying the anti-inflammatory and antitumour effects of isorhapontigenin: Insights from in vitro and in vivo studies. *Biomed. Pharmacother.* **180**, 117479. https://doi.org/10.1016/j.biopha.2024.117479 (2024).
11. Zhang, N. et al. Isorhapontigenin (ISO) inhibits EMT through FOXO3A/METTL14/VIMENTIN pathway in bladder cancer cells. *Cancer Lett.* **520**, 400–408. https://doi.org/10.1016/j.canlet.2021.07.041 (2021).
12. Zhu, C. et al. Isorhapontigenin induced cell growth inhibition and apoptosis by targeting EGFR-related pathways in prostate cancer. *J. Cell Physiol.* **233**, 1104–1119. https://doi.org/10.1002/jcp.25968 (2018).
13. Navarro-Orcajada, S. et al. Antiproliferative effects in colorectal cancer and stabilisation in cyclodextrins of the phytoalexin Isorhapontigenin. *Biomedicines* https://doi.org/10.3390/biomedicines11113023 (2023).
14. Subedi, L. et al. A Stilbenoid Isorhapontigenin as a potential anti-cancer agent against breast cancer through inhibiting sphingosine kinases/Tubulin Stabilization. *Cancers (Basel)* **11**, 1947. https://doi.org/10.3390/cancers11121947 (2019).
15. Xu, Z. et al. Isorhapontigenin suppresses growth of patient-derived glioblastoma spheres through regulating miR-145/SOX2/cyclin D1 axis. *Neuro. Oncol.* **18**, 830–839. https://doi.org/10.1093/neuonc/nov298 (2016).
16. Fang, Y. et al. Cyclin d1 downregulation contributes to anticancer effect of isorhapontigenin on human bladder cancer cells. *Mol. Cancer Ther.* **12**, 1492–1503. https://doi.org/10.1158/1535-7163.Mct-12-0922 (2013).
17. Zhao, L. et al. Network pharmacology, a promising approach to reveal the pharmacology mechanism of Chinese medicine formula. *J. Ethnopharmacol.* **309**, 116306. https://doi.org/10.1016/j.jep.2023.116306 (2023).
18. Torres, P. H. M., Sodero, A. C. R., Jofily, P. & Silva-Jr, F. P. Key topics in molecular docking for drug design. *Int. J. Mol. Sci.* https://doi.org/10.3390/ijms20184574 (2019).
19. Ogata, H. et al. KEGG: Kyoto Encyclopedia of Genes and Genomes. *Nucleic Acids Res.* **27**, 29–34. https://doi.org/10.1093/nar/27.1.29 (1999).
20. Kanehisa, M. Toward understanding the origin and evolution of cellular organisms. *Protein Sci.* **28**, 1947–1951. https://doi.org/10.1002/pro.3715 (2019).
21. Kanehisa, M., Furumichi, M., Sato, Y., Matsuura, Y. & Ishiguro-Watanabe, M. KEGG: biological systems database as a model of the real world. *Nucleic Acids Res.* **53**, D672-d677. https://doi.org/10.1093/nar/gkae909 (2025).
22. Chen, Y. et al. Effects of traditional Chinese medicine combined with chemotherapy for extensive-stage small-cell lung cancer patients on improving oncologic survival: Study protocol of a multicenter, randomized, single-blind, placebo-controlled trial. *Trials* **22**, 437. https://doi.org/10.1186/s13063-021-05407-1 (2021).
23. Wei, W. T. et al. Antitumor and apoptosis-promoting properties of emodin, an anthraquinone derivative from Rheum officinale Baill, against pancreatic cancer in mice via inhibition of Akt activation. *Int. J. Oncol.* **39**, 1381–1390. https://doi.org/10.3892/ijo.2011.1147 (2011).
24. Dong, X. et al. Aloe-emodin: A review of its pharmacology, toxicity, and pharmacokinetics. *Phytother. Res.* **34**, 270–281. https://doi.org/10.1002/ptr.6532 (2020).
25. Zheng, Q. et al. A novel STAT3 inhibitor W2014-S regresses human non-small cell lung cancer xenografts and sensitizes EGFR-TKI acquired resistance. *Theranostics* **11**, 824–840. https://doi.org/10.7150/thno.49600 (2021).
26. Li, J. et al. Urinary bisphenol A and its interaction with ESR1 genetic polymorphism associated with non-small cell lung cancer: Findings from a case-control study in Chinese population. *Chemosphere* **254**, 126835. https://doi.org/10.1016/j.chemosphere.2020.126835 (2020).
27. Harrison, P. T., Vyse, S. & Huang, P. H. Rare epidermal growth factor receptor (EGFR) mutations in non-small cell lung cancer. *Semin. Cancer Biol.* **61**, 167–179. https://doi.org/10.1016/j.semcancer.2019.09.015 (2020).
28. Attili, I. et al. SRC and PIM1 as potential co-targets to overcome resistance in MET deregulated non-small cell lung cancer. *Transl. Lung Cancer Res.* **9**, 1810–1821. https://doi.org/10.21037/tlcr-20-681 (2020).
29. Jiang, N. et al. Role of PI3K/AKT pathway in cancer: The framework of malignant behavior. *Mol. Biol. Rep.* **47**, 4587–4629. https://doi.org/10.1007/s11033-020-05435-1 (2020).
30. Sadrkhanloo, M. et al. New emerging targets in osteosarcoma therapy: PTEN and PI3K/Akt crosstalk in carcinogenesis. *Pathol. Res. Pract.* **251**, 154902. https://doi.org/10.1016/j.prp.2023.154902 (2023).
31. Asati, V., Bharti, S. K., Mahapatra, D. K., Asati, V. & Budhwani, A. K. Triggering PIK3CA mutations in PI3K/Akt/mTOR axis: Exploration of newer inhibitors and rational preventive strategies. *Curr. Pharm. Des.* **22**, 6039–6054. https://doi.org/10.2174/1381612822666160614000053 (2016).
32. Arafeh, R. & Samuels, Y. PIK3CA in cancer: The past 30 years. *Semin. Cancer Biol.* **59**, 36–49. https://doi.org/10.1016/j.semcancer.2019.02.002 (2019).
33. Woenckhaus, J. et al. Prognostic value of PIK3CA and phosphorylated AKT expression in ovarian cancer. *Virchows Arch.* **450**, 387–395. https://doi.org/10.1007/s00428-006-0358-3 (2007).
34. Wang, L. et al. Correction to: α2,6-Sialylation promotes immune escape in hepatocarcinoma cells by regulating T cell functions and CD147/MMP signaling. *J. Physiol. Biochem.* **75**, 619. https://doi.org/10.1007/s13105-019-00709-0 (2019).
35. Yu, M., Qi, B., Xiaoxiang, W., Xu, J. & Liu, X. Baicalein increases cisplatin sensitivity of A549 lung adenocarcinoma cells via PI3K/Akt/NF-κB pathway. *Biomed. Pharmacother.* **90**, 677–685. https://doi.org/10.1016/j.biopha.2017.04.001 (2017).
36. Tadesse, S. et al. Targeting CDK2 in cancer: Challenges and opportunities for therapy. *Drug Discov. Today* **25**, 406–413. https://doi.org/10.1016/j.drudis.2019.12.001 (2020).
37. Qie, S. & Diehl, J. A. Cyclin D1, cancer progression, and opportunities in cancer treatment. *J. Mol. Med. (Berl)* **94**, 1313–1326. https://doi.org/10.1007/s00109-016-1475-3 (2016).
38. Koerner, L. et al. NEMO- and RelA-dependent NF-κB signaling promotes small cell lung cancer. *Cell Death Differ.* **30**, 938–951. https://doi.org/10.1038/s41418-023-01112-5 (2023).

39. Gong, W. J. et al. Resistin facilitates metastasis of lung adenocarcinoma through the TLR4/Src/EGFR/PI3K/NF-κB pathway. *Cancer Sci.* **109**, 2391–2400. https://doi.org/10.1111/cas.13704 (2018).

Acknowledgements
We thank the distinguished investigators for generously publishing their research data on Isorhapontigenin and lung cancer. The authors thank J-WY and Y-FK for their enthusiastic help and selfless assistance in initiating this study.

Author contributions
Jiyong Wang and Yanfen Kang designed, guided and supervised the project. Zhiyu Wu and Chengyu Hou wrote the primary manuscript. Jiyong Wang and Yanfen Kang revised the manuscript. Chengyu Hou, Qiulin Zhu, Zixia Huang, conducted the experiments and Network pharmacology analysis. Zesheng Lu conducted molecular docking work and draw pictures, Chunhui Shen, Yanzhong Liu, Zhenhui Wang provide valuable suggestions and assistance for the experiment, bioinformatics analysis and manuscript writing.

Funding
This work was financially supported by the National Traditional Chinese Medicine Inheritance and Innovation Center, The First Affiliated Hospital of Guangzhou University of Chinese Medicine, China (Grant No.2022ZD08); Administration of Traditional Chinese Medicine of Guangdong Province, China (Grant No. 20241105); and Science and Technology Planning Project of Guangdong Province, China (Grant No.20221402).

Declarations

Competing interests
The authors declare no competing interests.

Additional information
Supplementary Information The online version contains supplementary material available at https://doi.org/10.1038/s41598-025-01648-1.

Correspondence and requests for materials should be addressed to Y.K. or J.W.